

of calculation, which weight the four independent measurements differently, are all consistent with the same mass value for a given event. (4) The masses obtained are not inconsistent with other independent measurements of the negative K -particle mass. Table III lists some other measurements of the K^- mass. These masses, along with the masses from the three scattering events of this paper, are consistent with a mass of 966 electron masses,⁵ the mass of the τ^+ particle. (5) Only on event 65 was it possible to make accurate ionization measurements on the K -track before and after the scattering. These measurements gave an energy change of $+5 \pm 10$ Mev which is inconsistent with a large energy loss at the point of scattering. It should also be noted that the 4-Mev proton from this event lies below the Coulomb barrier for the heavy elements in the emulsion.

Although the number of events is low, an estimate of

⁵ R. Haddock, Phys. Rev. **100**, 1803 (A) (1955).

the (K^-, p) elastic scattering cross section is of interest. Three scatterings in 560 cm of track analyzed in this experiment give a cross section of 170 millibarns. If additional length of track of other observers⁶ is included in which no (K^-, p) scatterings were observed, a cross section of 44 millibarns is obtained. This is in agreement with a geometric cross section for the (K^-, p) interaction. The ratio of the (K^-, p) cross section to the (K^+, p) cross section (~ 15 millibarns)⁷ is about 3 and is in agreement with the ratio of the cross sections for the K^- and K^+ interactions with nuclei in emulsion.

We wish to thank Irene Brown who found the three events, A. J. Oliver for processing the emulsion, and Dr. E. Lofgren and the Bevatron crew for their cooperation in the emulsion exposure.

⁶ Webb, Chupp, Goldhaber, and Goldhaber, 630 cm (to be published); J. Hornbostel and E. O. Salant, 136 cm, Phys. Rev. **102**, 502 (1956); D. M. Fournet and M. Widgoff, 868 cm Phys. Rev. **102**, 929 (1956).

⁷ Lannutti, Chupp, Goldhaber, Goldhaber, Helmy, Illoff, Pevsner, and Ritson, Phys. Rev. **101**, 1617 (1956).

Properties of Heavy Unstable Particles Produced by 1.3-Bev π^- Mesons*

R. BUDDE,[†] M. CHRETIEN, J. LEITNER, N. P. SAMIOS, M. SCHWARTZ,[‡] AND J. STEINBERGER
 Physics Department, Nevis Cyclotron Laboratories, Columbia University, Irvington-on-Hudson, New York

(Received June 15, 1956)

A propane bubble chamber has been exposed to a π^- beam of 1.3-Bev kinetic energy. The reactions

$$\begin{aligned}\pi^- + p &\rightarrow \Sigma^- + K^+, \\ \pi^- + p &\rightarrow \Lambda^0 + \theta^0, \\ \pi^- + p &\rightarrow \Sigma^0 + \theta^0,\end{aligned}$$

can be experimentally distinguished from carbon events. Results based on the first 55 such events are presented. The center-of-mass production distribution of the Σ^- is peaked forward, that of the Λ^0 backward. No large anisotropies in the angular correlation of production and decay were found, so that we have no evidence for spin in excess of $\frac{1}{2}$ for any of the three particles: Σ^- , Λ^0 , or θ^0 . A study of the relative abundance of single and double V production indicates that both Λ^0 and θ^0 have either long-lived "states" or neutral decay modes. A statistical analysis gives $\bar{\alpha}_{\Lambda^0} = 0.3_{-0.12}^{+0.15}$, $\bar{\alpha}_{\theta^0} = 0.3_{-0.12}^{+0.19}$, for the normal charged decay probabilities ($\Lambda^0 \rightarrow \pi^- + p$; $\theta^0 \rightarrow \pi^+ + \pi^-$) of the Λ^0 and θ^0 , respectively. One event was analyzed to obtain the energy released in Σ^- decay. $\Sigma^- \rightarrow \pi^- + n + Q$; $Q = 118 \pm 2.6$ Mev. The Σ^- lifetime on the basis of 16 decays is $(1.4_{-0.5}^{+1.0}) \times 10^{-10}$ sec.

I. INTRODUCTION

THE production of strange particles by high-energy mesons in hydrogen has been studied by Fowler, Shutt, Thorndike, and Whittemore¹ in a diffusion cloud chamber. It was this experiment which demonstrated that hyperons and K mesons are produced in accordance

with the hypothesis of associated production.^{2,3} A similar study, at lower energy, was made by Walker and Shephard.⁴ In total, 14 events have been observed, 9 by the Brookhaven group at ~ 1.5 Bev and 5 by the Wisconsin group at ~ 1 Bev. We present here preliminary results from an exposure of a liquid propane bubble chamber to a 1.3-Bev (kinetic energy) π^- beam at Brookhaven.

* This research is supported in part by the joint program of the Office of Naval Research and the U. S. Atomic Energy Commission. Reproduction in whole or in part is permitted for any purpose of the U. S. Government.

[†] On leave from CERN Laboratories, Geneva, Switzerland.

[‡] National Science Foundation Fellow.

¹ Fowler, Shutt, Thorndike, and Whittemore, Phys. Rev. **98**, 121 (1954).

² M. Gell-Mann and A. Pais, *Proceedings of the Fifth Annual Rochester Conference on High Energy Physics*, 1955 (Interscience Publishers, Inc., New York, 1955).

³ T. Nakano and K. Nishijima, Progr. Theoret. Phys. Japan **10**, 581 (1953).

⁴ W. Walker and W. Shephard, Phys. Rev. **101**, 1810 (1954).

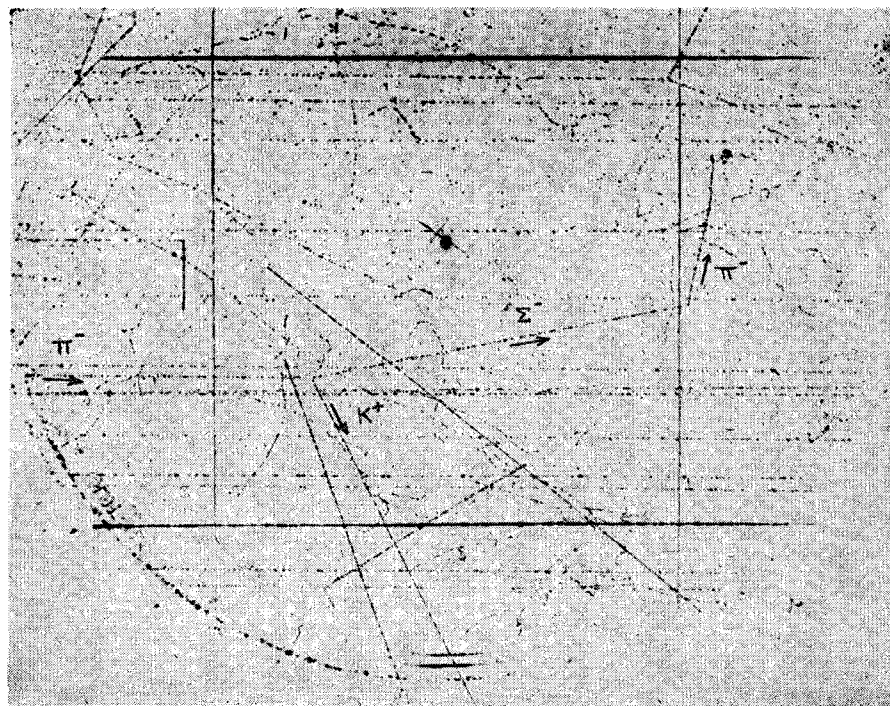


FIG. 1. $\pi^- + p \rightarrow \Sigma^- + K^+$, $\Sigma^- \rightarrow \pi^- + n$. The Σ^- decay product stops in the chamber and makes a star which shows a short proton recoil. It is therefore identified as a π^- .

In particular, we report here results based on the observation of 55 strange-particle production events in hydrogen (described in Tables I, II). These data are only the beginning of a much larger body of information expected in the near future with the continued utilization of bubble chambers. Considerably larger chambers will soon be in use, and one might hope to see several hundreds of such events. A more complete report on the experimental methods and more extensive results will appear later. The results described below include information on: (1) production angular distributions; (2) decay angular correlations; spins of the strange particles; (3) lifetimes and alternate decay modes; and (4) Q value for Σ^- decay.

II. EXPERIMENTAL CONDITIONS

The chamber is $6\frac{1}{8}$ in. in diameter and 4 in. deep. By using dark-field photographic technique, two views are taken with a stereoscopic angle of 0.25 radian. There is no magnetic field. The propane is kept at a temperature of 57.5°C and a pressure of 340 psi before expansion. The density of expanded propane is 0.43 g/cm^3 ; the hydrogen density is 0.078 g/cm^3 , which is slightly larger than the density of liquid hydrogen. The incident beam is carefully collimated and magnetically analyzed in such a way that the spread in beam energy deduced from the plotted trajectories is $\pm 1\%$. The absolute value of the pion beam momentum is $1.433 \pm 0.015\text{ Bev}/c$, as will be shown later. The exposure of 35 effective hours produced a total of $\sim 25\,000$ pictures, with an average of ~ 15 tracks per picture.

III. IDENTIFICATION OF EVENTS

Identification of various production events is based on the kinematics of the reactions

- (1) $\pi^- + p \rightarrow \Sigma^- + K^+$,
- (2) $\pi^- + p \rightarrow \Lambda^0 + \theta^0$,
- (3) $\pi^- + p \rightarrow \Sigma^0 + \theta^0$, $\Sigma^0 \rightarrow \Lambda^0 + \gamma$.

The assignment of charge in reaction (1) is based on the ideas of Gell-Mann,⁵ which have been most fruitful in the correlation of strange particle processes. According to these views, the process $\pi^- + p \rightarrow \Sigma^+ + K^-$, which is indistinguishable from (1) in our experiment, is forbidden. The events of reaction (1) appear as 2-prong stars produced by the incident π^- . In order that a two-prong star be classified as a $\Sigma^- - K^+$ production event, it must satisfy the following criteria:

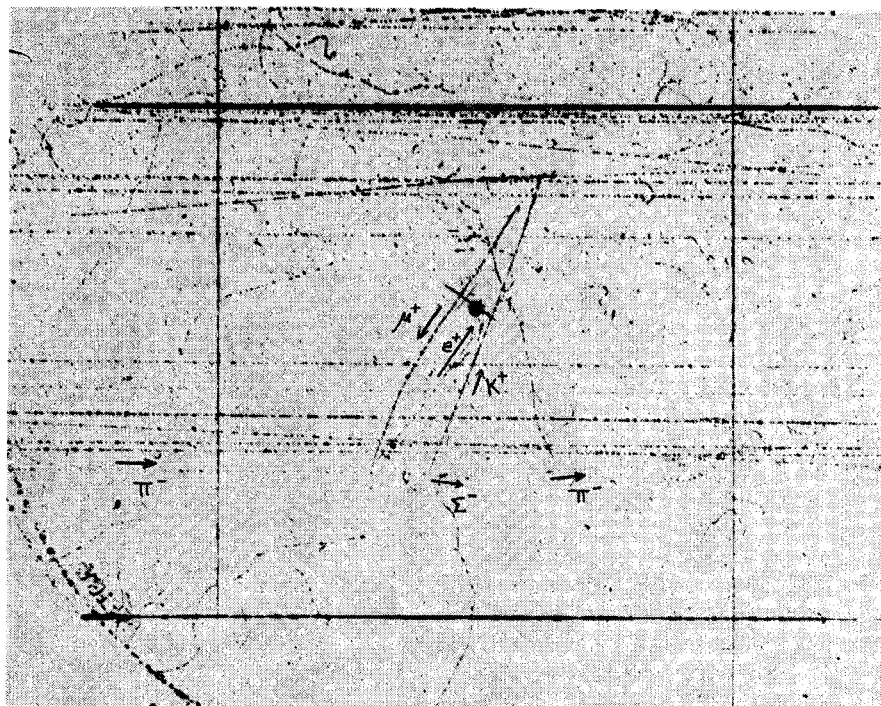
1. The three tracks must be coplanar.
2. The angles of the tracks must be consistent with the known reaction kinematics.
3. The bubble densities and multiple scatterings of tracks must be consistent with those expected for K 's and Σ 's at the observed angles.
4. The ranges of any stoppings in the liquid must be consistent with those expected from the kinematics.
5. At least one of the secondaries must show a decay in the chamber.

Examples of such events are shown in Figs. 1 to 3.

Each projected angle is usually measured with an accuracy of $\sim \pm 0.3^\circ$; this results in an error of $\sim \pm 1^\circ$ in the calculated space angle. The bubble density and

⁵ M. Gell-Mann (to be published).

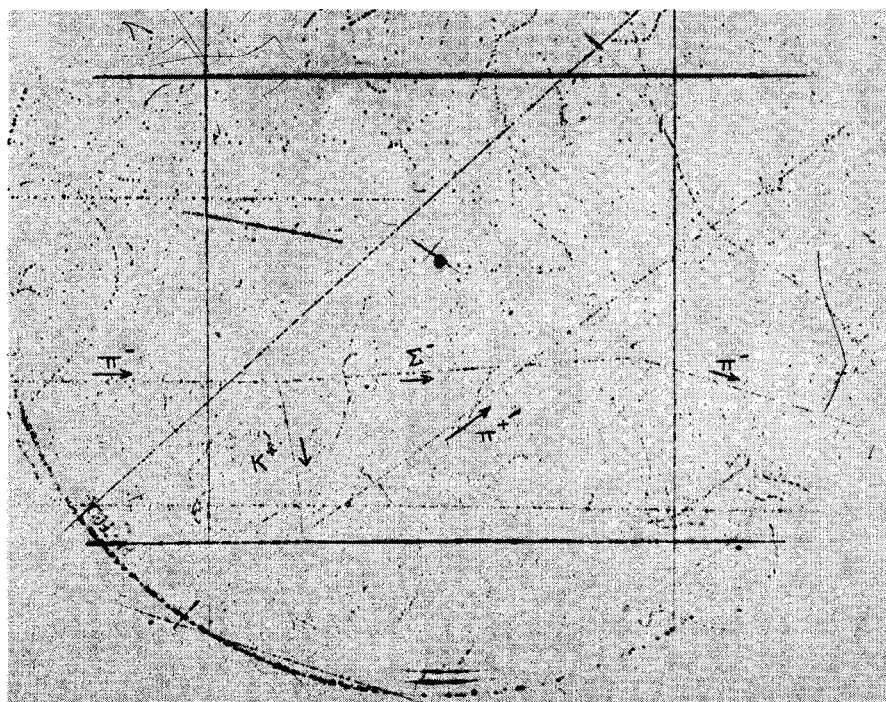
FIG. 2. $\pi^- + p \rightarrow \Sigma^- + K_{\mu 3}^+$. here both the Σ^- and K^+ decay. The K^+ decay product itself decays into an electron, and is therefore identified as a μ^+ .



scattering criteria are used only qualitatively. Since approximately half the total proton cross section in the chamber is contributed by carbon protons, the possibility that some of the events reported here are grazing collisions in carbon, rather than collisions with free protons, must be considered. To obtain an estimate of

the number of such quasi-elastic events, some 1200 two-prong stars were systematically studied. In particular they were scrutinized for a possible diffuse grouping about the $\pi-p$ elastic scattering angular correlation curve, since the Fermi momentum of a struck carbon proton should give rise to momentum unbalances of the

FIG. 3. $\pi^- + p \rightarrow \Sigma^- + K_{e 3}^+$. The K^+ decay product is minimum-ionizing and scatters severely, and is therefore identified as an electron. The electron was erroneously labeled π^+ and should read e^+ .



order of ~ 550 Mev/ c or angular deviations of the order of $\sim 10^\circ$. The results of this study, together with the hydrogen elastic scattering data, will be reported in more detail later. We content ourselves here with the statement that, of the 1200 stars, 660 were identified as π - p elastic collisions within the precision of our measurements and that the remainder showed no diffuse grouping about the π - p kinematics. We feel that the background, extended into our region of acceptance for π - p productions, can contribute at most ~ 10 events, and consequently the carbon contamination is entirely negligible. In the case of $\Sigma^- - K^+$ production the selection criteria are equally precise, so that the carbon contamination in the 17 events found is probably much less than a single event. In the case of $\Lambda^0 - \theta^0$ production the selection criteria are usually not so restrictive to background. We feel, however, that here too the carbon contamination can contribute at most 2 or 3 of the 37 events reported. The measurement accuracy for these events will be discussed in more detail later.

We have found, to date, 17 examples of the reaction $\pi^- + p \rightarrow \Sigma^- + K^+$. Of these, 16 show the decay of the Σ^- in flight. In 5 events the decay product of the K^+ appears in the chamber. In three of these cases the secondary is a fast, lightly ionizing particle; in one case (Fig. 2) the K^+ stops in the top glass quite close to the liquid surface, and the decay product reappears in the chamber and stops with the emission of an electron. The secondary is, therefore, a μ meson of about 20 Mev. This is, then, an example of the production of a $K_{\mu 3}^+$ in

hydrogen. In another event (Fig. 3) the K^+ stops in the chamber emitting a minimum track which scatters severely and is, therefore, identified as an electron. The momentum of this secondary is ~ 40 Mev/ c . This is an example of $K_{e 3}^+$ production in hydrogen. In two cases the K^+ suffers a nuclear collision before stopping. In both of these the K^+ is quite slow. In one case the scattering is without visible recoil and is therefore in carbon. In the other case the K^+ with a residual energy of ~ 10 Mev scatters on a proton. No scatterings of the Σ^- were observed, and no Σ^- stars were observed in a total path of 37.7 g/cm 2 of propane. No events were found which were incompatible with the assumed charge assignment for the Σ and K .

Events of reaction (2) appear as mesons stopping in the chamber with the appearance of one or two V 's formed by the decay products of the neutral unstable particles. Examples are shown in Figs. 4 and 5. If only one V appears, we require that the two tracks of the V decay be coplanar with the line of flight of the neutral particle; i.e., the line joining the end of the stopping π^- and the vertex of the V . In addition, the angles of the $\Lambda^0(\theta^0)$ decay products determine the energy of the $\Lambda^0(\theta^0)$ if one makes use of the well-known Q values for these reactions.⁶ The energy measured in this way must then agree with that expected on the basis of the observed $\Lambda^0(\theta^0)$ production angle and known production kinematics. In the event that two V 's are observed, since the above procedure is applicable for each V , the event is well overdetermined. Furthermore, it is re-

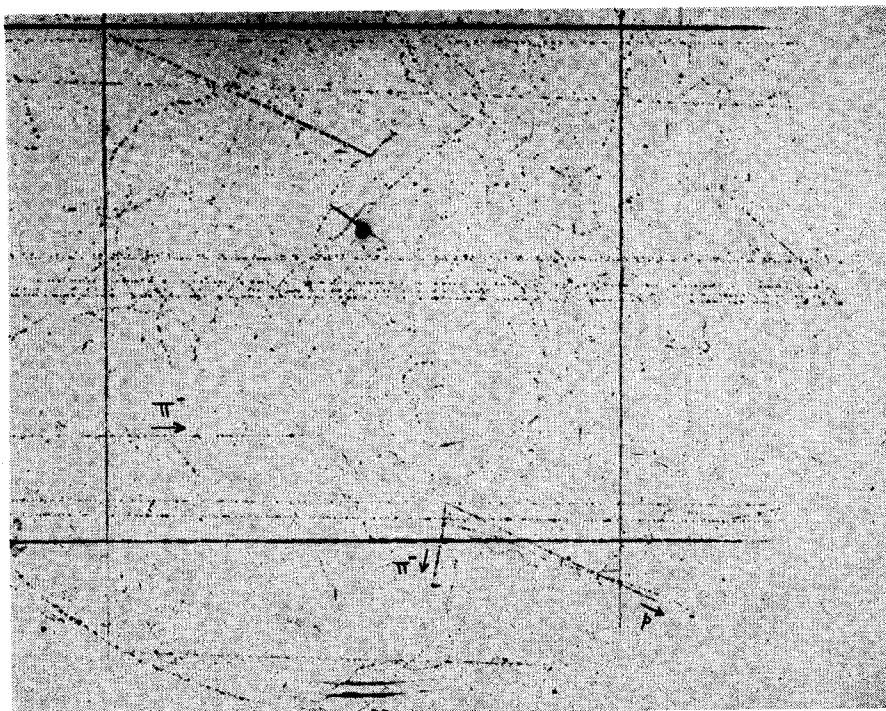
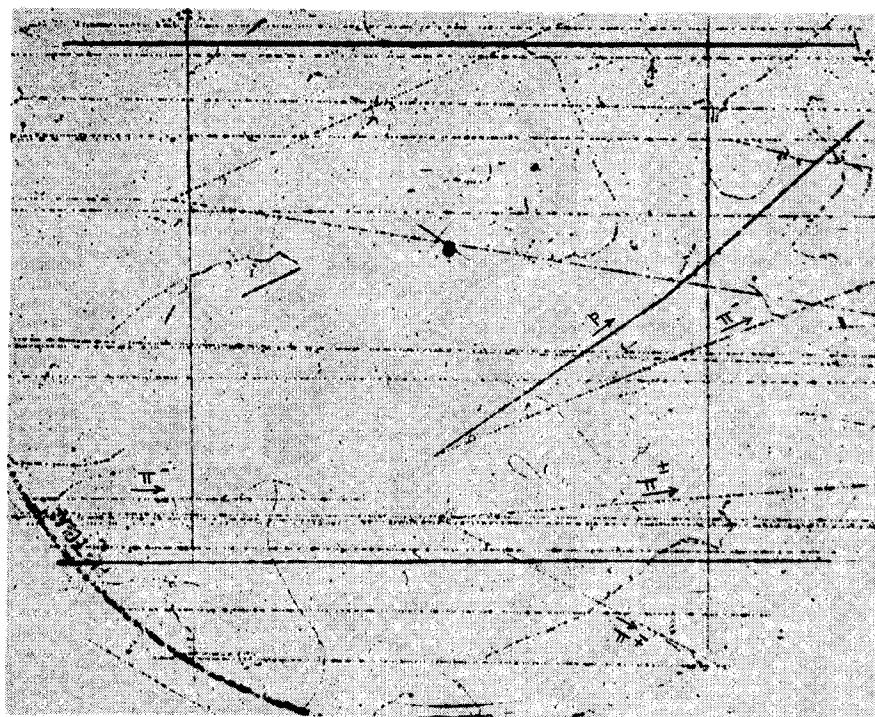


FIG. 4. A $\Lambda^0 - \theta^0$ production in which only a single V is seen. The V is identified as a Λ^0 and shows a slow π^- producing a star.

⁶ R. W. Thompson, "International Congress on Elementary Particles, Pisa, July, 1955," Nuovo cimento (to be published).

FIG. 5. A Λ^0 - θ^0 production in which both V 's are seen. The Λ^0 shows, characteristically, a heavily ionizing proton and a minimum-ionizing π^- . The θ^0 shows two minimum-ionizing π 's.



quired that the bubble densities, multiple scattering, and the ranges of the secondaries, when available, be consistent with the kinematics of the reaction. In judging the precision of the method, it should be kept in mind that the end of the incident π^- is not precisely defined because of the finite bubble density. The probable error in position due to this effect is $\sim \frac{1}{2}$ mm. The average Λ^0 and θ^0 path length is ~ 2 -3 cm, but those with path lengths of the order of a few mm are not measured with good precision. The usual accuracy in the determination of the energy of the Λ^0 and θ^0 is ~ 5 -15%.

The evidence for the existence of a Σ^0 with a mass near that of the Σ^+ is still not conclusive. However, there are strong theoretical reasons⁵ to postulate this particle and its decay in a very short time ($\sim 10^{-20}$ sec) into a γ ray and Λ^0 with a Q of approximately 70 Mev. In our pictures this production event would appear almost identical to reaction (2) (since the Σ^0 would decay at the origin), but with the following differences:

1. If a θ^0 appears, for a given angle of appearance the kinetic energy would be lower than that in a Λ^0 - θ^0 production event by an amount which varies from $\sim 20\%$ at small production angles to $\sim 50\%$ at larger ones.
2. If a Λ^0 appears, its energy is not uniquely determined by the production angle. It can, in fact, have a reasonably large spread depending upon the angle of emission of the γ ray.

Of the 38 events in categories (1) and (2), only 4 exhibit both V 's in the chamber; 3 of these fit Λ^0 - θ^0 production well, the fourth fits well for Σ^0 - θ^0 production

and does not seem reconcilable with (2). The remaining 34 events consist of only one observed V . Of these, 19 are Λ^0 's and 15 are θ^0 's. In these categories, 15 events cannot be measured well enough to distinguish Λ^0 and Σ^0 production confidently. 17 others are definitely identifiable as Λ^0 - θ^0 production, and only 2 events exist for which Σ^0 production seems definitely indicated. Both the latter are events in which a θ^0 was observed; no events in which a single Λ^0 was seen can be unambiguously interpreted as Σ^0 - θ^0 production.

IV. BEAM ENERGY

The most accurate determination of the beam energy utilizes two events of the type $\pi^- + p \rightarrow \Sigma^- + K^+$ in which the K^+ comes to rest without nuclear interaction. Using mass values $M_{\Sigma^-} = 2344m_e$ ⁷ and $M_{K^+} = 965.5m_e$ ⁸, we find for the beam momentum in the 2 cases, $P_{\pi} = 1.420 \pm 0.005$ Bev/c and $P_{\pi} = 1.447 \pm 0.005$ Bev/c, respectively; these yield a mean momentum $P_{\pi} = 1.433 \pm 0.015$ Bev/c. The latter error indicates the beam momentum spread determined from the calculated trajectories.

V. PRODUCTION ANGULAR DISTRIBUTIONS

The center-of-mass distributions for the 38 events which are either Λ^0 - θ^0 or Σ^0 - θ^0 production are presented together in Fig. 6. In the same figure the center-of-mass angles of the seventeen $\Sigma^- - K^+$ events are also shown.

⁷ Chupp, Goldhaber, Goldhaber, and Webb, "Proceedings of the International Conference on Elementary Particles, Pisa, 1955," Nuovo cimento (to be published).

⁸ Heckman, Smith, and Barkas, University of California Radiation Laboratory Report UCRL-3156, 1955 (unpublished).

TABLE I. A compilation of the data concerning the production events $\pi^- + p \rightarrow \Lambda^0 + \theta^0$ and $\pi^- + p \rightarrow \Sigma^0 + \theta^0$. p is the laboratory momentum of the observed particle in Bev/c. θ is the polar angle and ϕ the azimuthal angle in a coordinate system in which the decaying particle is at rest (see Fig. 7). β is the production angle of the heavy meson in the center-of-mass system of the π^- , p . The last column indicates the nature of the event. (1) \equiv sure $\Lambda^0 - \theta^0$; (2) \equiv either Λ^0 or Σ^0 ; (3) \equiv very likely $\Sigma^0 - \theta^0$.

Observed particle	Unobserved particle	Observed path length cm	Potential path length -0.5 cm	p/mc	ϕ	θ	β	Σ^0 or Λ^0
Λ^0		0.60	4.65	0.94	46°	103°	92°	(2)
	θ^0		2.50	1.46				
	Λ^0		6.55	0.45			37°	(2)
θ^0		3.90	7.20	1.95	230°	103°		
Λ^0		0.65	10.85	0.29	217°	112°	15°	(2)
	θ^0		10.60	2.36				
Λ^0		1.60	5.95	0.47	114°	96°	40°	(1)
	θ^0		2.50	2.13				
	Λ^0		7.80	0.29			15°	(1)
θ^0		5.80	10.15	2.25	314°	139°		
Λ^0		1.20	9.20	0.45	212°	60°	38°	(1)
θ^0		1.20	6.25	2.18	254°	112°		
	Λ^0		9.10	0.88			91°	(2)
θ^0		0.40	8.95	1.46	259°	150°		
	Λ^0		12.15	0.26			11°	(1)
θ^0		10.60	10.80	2.29	207°	131°		
	Λ^0		8.15	0.40			31°	(2)
θ^0		3.05	9.75	2.07	166°	104°		
Λ^0		0.20	2.50	0.45	24°	53°	38°	(2)
	θ^0		3.80	2.02				
Λ^0		0.65	12.85	0.35	48°	24°	22°	(1)
	θ^0		11.00	2.25				
	Λ^0		11.00	0.32			18°	(1)
θ^0		2.65	8.90	2.23	19°	142°		
Λ^0		2.45	3.95	0.32	280°	39°	10°	(2)
	θ^0		3.60	2.23				
	Λ^0		5.50	1.61			139°	(2)
θ^0		0.47	5.50	0.53	158°	115°		
	Λ^0		10.75	0.85			76°	(3)
θ^0		1.45	7.20	1.53	293°	142°		
	Λ^0		4.45	0.70			67°	(1)
θ^0		0.85	4.50	1.88	125°	114°		
Λ^0		1.20	4.65	0.42	288°	69°	25°	(2)
θ^0		7.75	10.30	2.11	283°	117°		
Λ^0		0.90	2.45	0.55	201°	106°	50°	(2)
	θ^0		1.85	1.93				
Λ^0		0.1	6.75	0.76	344°	80°	72°	(2)
	θ^0		11.00	1.75				
Λ^0		6.45	11.50	0.85	145°	105°	81°	(1)
	θ^0		5.40	1.48				
	Λ^0		3.35	1.10			34°	(1)
θ^0		7.40	11.45	2.11	158°	102°		
	Λ^0		6.90	0.72			67°	(1)
θ^0		5.15	7.55	1.86	2°	99°		
Λ^0		4.10	5.35	0.93	244°	121°	89°	(2)
	θ^0		9.80	1.48				
Λ^0		0.2	4.00	0.55	312°	82°	53°	(1)
θ^0		3.45	7.30	2.00	351°	165°		
Λ^0		2.40	4.60	1.21	186°	65°	117°	(1)
	θ^0		3.05	0.83				
Λ^0		0.65	2.05	0.26	260°	78°	10°	(1)
	θ^0		2.05	2.18				
	Λ^0		12.45	0.26			16°	(1)
θ^0		7.50	12.55	2.11	34°	110°		
Λ^0		5.35	6.70	0.38	207°	111°	26°	(1)
	θ^0		7.35	2.23				
Λ^0		4.05	6.85	1.13	287°	140°	117°	(1)
	θ^0		12.00	0.98				
	Λ^0		2.00	0.76			72°	(1)
θ^0		1.60	6.65	1.72	222°	136°		
Λ^0		2.25	5.65	0.69	139°	155°	68°	(1)
	θ^0		9.25	1.88				
	Λ^0		7.40	0.51			36°	(3)
θ^0		0.43	8.50	1.88	197°	105°		
Λ^0		0.25	4.50	0.40	268°	88°	30°	(2)
	θ^0		2.80	2.20				
Λ^0		2.70	5.20	0.38	51°	34°	25°	(2)
	θ^0		5.55	2.23				
Λ^0		2.52	7.70	0.40	270°	115°	37°	(3)
θ^0		2.95	3.05	2.11	193°	165°		
Λ^0		6.65	12.60	1.10	222°	96°	114°	(2)
	θ^0		5.70	1.07				
Λ^0		0.25	8.00	0.90	224°	133°	85°	(2)
	θ^0		4.60	1.53				

Needless to say, the statistics are quite poor; it is, however, strongly indicated that in Λ^0 production the heavy meson is emitted preferentially well forward, whereas in Σ^- production, the heavy meson is emitted preferentially backward. For comparison, the function $(\cos\theta_K+1)^2$ is also plotted. This represents the most peaked angular distribution which can be obtained with only s and p waves. It seems fairly clear that higher orbital momenta make an appreciable contribution to the final states. Since the c.m. momentum of the hyperons or heavy mesons is approximately ~ 200 Mev/c, the interaction radius must be at least of the order of $\hbar/p \approx 2 \times 10^{-13}$ cm.

VI. ANGULAR CORRELATIONS IN PRODUCTION AND DECAY: SPINS OF Λ^0 , θ^0 , AND Σ^-

If the Λ^0 , θ^0 , or Σ^- have spin greater than $\frac{1}{2}$, and if, furthermore, this spin is polarized in the production

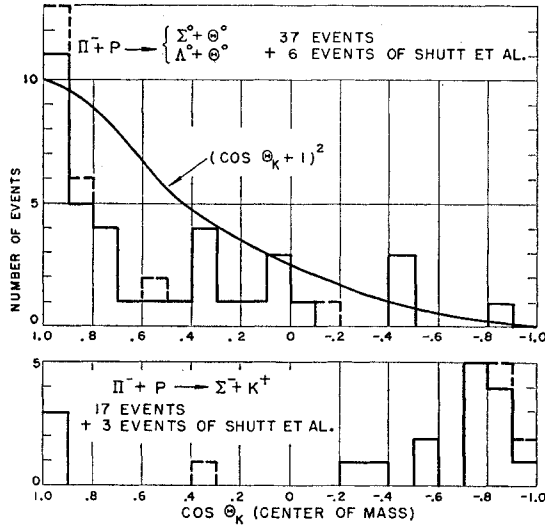


FIG. 6. The production angular distribution for the reactions $\pi^- + p \rightarrow \Lambda^0 + \theta^0$, $\pi^- + p \rightarrow \Sigma^- + K^+$. θ_K is the center-of-mass angle of the heavy mesons in each case. The sixth Shutt event should be inserted between .8 and .7.

process, then this polarization appears experimentally in the form of anisotropies in the angles relating the production and decay process. Figure 7 is a diagram of the kinematical situation. We take as coordinate system the system in which the decaying particle is at rest, with the direction of the transformation velocity as z axis and the normal to the production plane (invariant under the transformation from the laboratory system to this system) as x axis. The angular correlation information is then exhausted if both the polar and azimuthal angles θ and ϕ of one of the two decay products, say the π^- meson, are given. The azimuthal angle ϕ differs from the (invariant) dihedral angle between decay and production planes by $\pi/2$. The experimental data are given in Tables I and II. A complete presentation of the information unfortunately requires

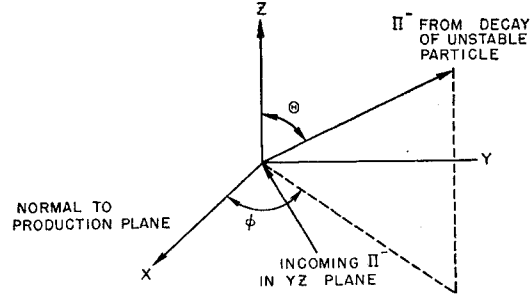


FIG. 7. The coordinate system in which the decaying unstable particle is at rest. The Z axis is taken in the direction of the laboratory to rest-frame transformation velocity.

simultaneous presentation of three angles: the production angle β and the two decay angles θ and ϕ . If one or two of them are integrated out, there is, of course, the danger of masking whatever anisotropies are present. However, with only of the order of 20 events, a three-dimensional presentation can hardly exhibit significant trends. Consequently, in Figs. 8 to 10 the data are plotted after integration over β . On the edges of the figures are histograms which are obtained after integration over one of the two remaining angles. We cannot distinguish between π^+ and π^- in θ^0 decay. The $\cos\theta$ plot here extends, therefore, only from $\pi/2$ to π .

If parity is a good quantum number in production and decay of the strange particles, then the distributions in ϕ and θ must exhibit symmetry about 90° (and 180°), i.e., $f(\theta) = f(\pi - \theta)$, and $g(\phi) = g(\pi - \phi) = g(2\pi - \phi)$. However, in view of the difficulty in understanding the equality of the lifetime and mass of $K_{\pi 2}$ and $K_{\pi 3}$ despite a difference in parity,^{9,10} it may be better to present all data until the assumption of parity conservation in decay is more

TABLE II. A compilation of the data concerning the reaction $\pi^- + p \rightarrow \Sigma^- + K^+$. Notation is identical to that of Table I. $K_L^+ \equiv K^+$ with lightly ionizing secondary.

Observed decays	Actual path of Σ^- (cm)	Pot. path of Σ^- (cm)	p/mc (Σ^-)	ϕ (Σ^- decay)	θ (Σ^- decay)	β	Nature of K^+
K^+			1.20			152°	K_L^+
Σ^-, K^+	5.5	9.2	1.15	125°	123°	135°	K_L^+
Σ^-	2.1	6.9	0.97	77°	97°	105°	
Σ^-	0.8	9.8	1.00	156°	108°	109°	
Σ^-	1.1	4.2	0.40	116°	41°	21°	
Σ^-, K^+	5.1	10.2	1.18	89°	152°	144°	K_L^+
Σ^-	0.37	2.9	1.14	79°	76°	135°	
Σ^-	3.2	9.1	1.14	35°	81°	132°	
Σ^-, K^+	6.0	9.4	1.21	270°	91°	152°	K_{s3}^+
Σ^-	2.0	4.9	1.08	28°	76°	126°	
Σ^-, K^+	1.7	9.1	1.18	116°	77°	147°	K_L^+
Σ^-, K^+	0.65	6.8	1.19	224°	45°	150°	$K_{\mu 3}^+$
Σ^-	0.48	8.6	0.37	107°	35°	18°	
Σ^-	0.33	2.9	0.37	233°	107°	14°	
Σ^-	6.3	8.9	1.14	2°	156°	136°	
Σ^-	3.6	5.4	1.16	124°	48°	137°	
Σ^-	4.6	5.5	1.11	33°	52°	123°	

⁹ Orear, Harris, and Taylor (to be published).

¹⁰ Feld, Odian, Ritson, and Wattenberg, Phys. Rev. **100**, 1539 (1955).

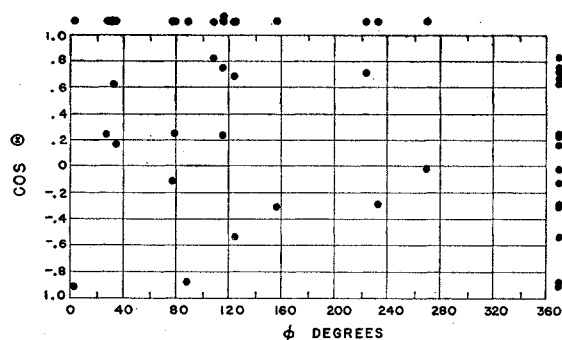


FIG. 8. Angular correlation plot of the cosine of the polar angle against the azimuthal angle ϕ for the reaction $\pi^- + p \rightarrow \Sigma^- + K^+$, $\Sigma^- \rightarrow \pi^- + n$. The point histograms on the edges of the figure represent the data after integration over the other coordinate.

clearly demonstrated. In fact, the data may be used to check this hypothesis, since any experimentally established violation of the symmetries above must be attributed to a lack of parity conservation.¹¹

In Fig. 11 we show the dihedral angles in the range 0° – 90° , after making use of the above symmetry properties. These may be compared with the results reported by Fowler *et al.* and Walker *et al.*, on the basis of eight Λ^0 events, six θ^0 events, and three Σ^- events. There is no indication of polarization in θ^0 production. However, the earlier results in the case of Λ^0 production in hydrogen show all eight events with dihedral angles between 0° and 45° . Twelve of our 23 events in which a Λ^0 was seen have dihedral angles in the same region. The combination of all these thirty-one Λ^0 , Σ^0 production events in hydrogen gives

$$N(0^\circ-45^\circ)/N(45^\circ-90^\circ) = 20/11.$$

We believe that the statistics are not adequate to demonstrate a polarization effect. For the Σ^- , the ratio is

$$N(0^\circ-45^\circ)/N(45^\circ-90^\circ) = 10/6;$$

here again statistics are inadequate to establish polarization.

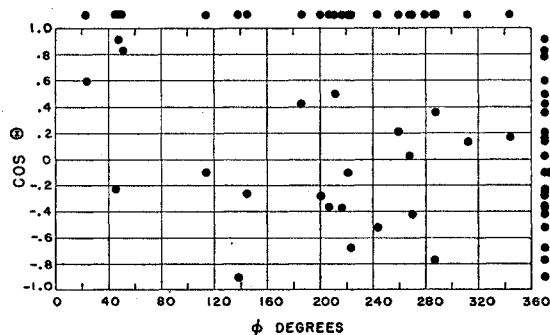


FIG. 9. Angular correlation plot for the reaction $\pi^- + p \rightarrow \Lambda^0 + \theta^0$, $\Lambda^0 \rightarrow \pi^- + p$.

¹¹ We wish here to acknowledge some very helpful discussions with T. D. Lee on these questions, and a communication from R. Karplus.

Adair¹² has pointed out that for the production angle β near zero or 180° , and assuming the spin of the θ^0 (or K^+) to be zero, the angular distribution in θ of the Λ^0 (or Σ^-) decay is determined by angular momentum and parity conservation alone. For example, for the spin of the hyperon $\frac{1}{2}$, the distribution in θ is isotropic, for spin $\frac{3}{2}$ it is $\frac{3}{2} \cos^2 \theta + \frac{1}{2}$, etc.

We have calculated the likelihood functions for these distributions, using those eleven Λ^0 and eight Σ^- events with $|\cos \beta| \geq 0.78$.

$$\text{For the } \Lambda^0: \frac{L_{\frac{3}{2}}(\theta)}{L_{\frac{1}{2}}(\theta)} = \prod_{i=1}^N \frac{(\frac{3}{2} \cos^2 \theta_i + \frac{1}{2})}{1} = 0.28.$$

$$\text{For the } \Sigma^-: \frac{L_{\frac{3}{2}}(\theta)}{L_{\frac{1}{2}}(\theta)} = 0.80.$$

For greater assumed spin j , the likelihood functions L_j would become progressively smaller. There is certainly no evidence here that the hyperon spins are larger than $\frac{1}{2}$; the best agreement is obtained with spin $\frac{1}{2}$.

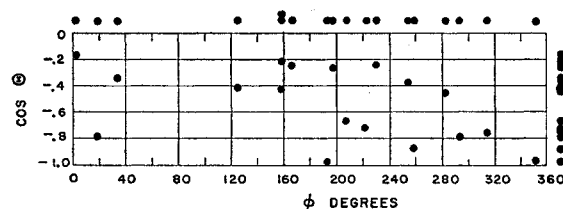


FIG. 10. Angular correlation plot for the reaction $\pi^- + p \rightarrow \Lambda^0 + \theta^0$, $\theta^0 \rightarrow \pi^+ + \pi^-$. The θ variation extends from $\pi/2$ to π since the π^+ and π^- are indistinguishable in this experiment.

for both Λ^0 and Σ^- . The data are still inadequate, but this kind of analysis seems promising.

VII. ANOMALOUS Λ^0 OR θ^0 PARTICLES

It is the underlying hypothesis of this paper, insofar as concerns neutral unstable particle production, that the observation of a single decay establishes the event. The trajectory and momentum of the unobserved particle can then be obtained from the kinematics, and as seen in Table I, the potential path of the unobserved particle has also been measured. The potential path is defined as the length of path the particle would have had, if it had not decayed, minus $\frac{1}{2}$ cm; the latter being approximately the length of decay tracks necessary to detect the decay.

It is then possible to ask: given a Λ^0 (θ^0) which is identified as coming from the process $\pi^- + p \rightarrow \Lambda^0 + \theta^0$, are the number of θ^0 's (Λ^0 's) observed with these Λ^0 's (θ^0 's) compatible with the known potential path lengths and the known lifetimes? We have observed only four double events despite the fact that the average potential path is of the order of the average mean free path both

¹² R. K. Adair, Phys. Rev. 100, 1540 (1955).

for Λ^0 and θ^0 decay. The answer is therefore negative in both cases. We have no *additional* information on the reason for the failure to observe the particles. They may escape detection either because of the existence of long-lived "states" of the θ^0 (Λ^0) or because of neutral decay modes.

Let α be the fraction of the Λ^0 (θ^0) particles which undergo normal charged decay, $1-\alpha$ the fraction which is either long-lived or has a neutral decay. One can then calculate the likelihood function,

$$L(\alpha) = \prod_{i=1}^M \frac{\alpha e^{-t_i/\tau}}{\tau} \prod_{j=M+1}^N [\alpha e^{-T_j/\tau} + 1 - \alpha],$$

for seeing, in N situations in which the Λ^0 (θ^0) of the reaction is observed, that M particles decay at the times t_1, t_2, \dots, t_M , and the remaining $N-M$ particles disappear without detection in potential path lengths with times $T_{M+1}, T_{M+2}, \dots, T_N$. τ is the mean life for θ^0 (Λ^0)

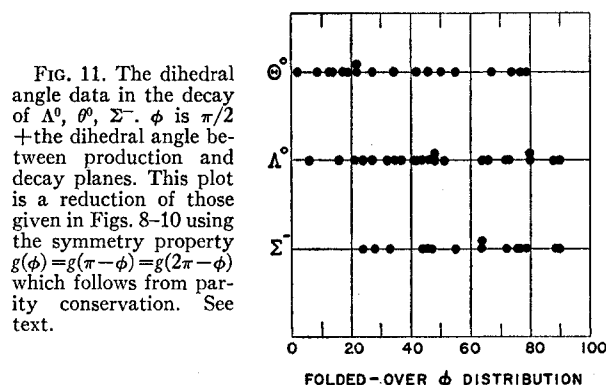


FIG. 11. The dihedral angle data in the decay of Λ^0 , θ^0 , Σ^- . ϕ is $\pi/2$ + the dihedral angle between production and decay planes. This plot is a reduction of those given in Figs. 8-10 using the symmetry property $g(\phi) = g(\pi - \phi) = g(2\pi - \phi)$ which follows from parity conservation. See text.

decay. We have taken

$$\tau_{\theta^0} = 1.25 \times 10^{-10} \text{ sec},^{13,14}$$

$$\tau_{\Lambda^0} = 3.0 \times 10^{-10} \text{ sec},^{13,15}$$

as the weighted best values of the θ^0 , Λ^0 lifetime data. The likelihood function $L(\alpha)$ is plotted vs the charged decay branching ratio α in Fig. 12 for the Λ^0 and in Fig. 13 for the θ^0 . The best values of α , $\bar{\alpha}_i$, along with statistical errors obtained from the width of $L(\alpha)$ at half-maximum are

$$\bar{\alpha}_{\Lambda^0} = 0.3_{-0.12}^{+0.15},$$

$$\bar{\alpha}_{\theta^0} = 0.3_{-0.12}^{+0.19}.$$

In considering the reliability of $\bar{\alpha}_{\Lambda^0(\theta^0)}$ it must be kept in mind that it depends upon the choice of lifetime. This dependence has been investigated. The uncertainty in $\bar{\alpha}_{\Lambda^0(\theta^0)}$ due to the experimental uncertainty in the Λ^0 (θ^0)

¹³ D. Gayther, Phil. Mag. 45, 570 (1954).

¹⁴ Blumenfeld, Chinowsky, Lederman, and Booth, Phys. Rev. 102, 1184 (1956).

¹⁵ D. I. Page, Phil. Mag. 45, 863 (1954).

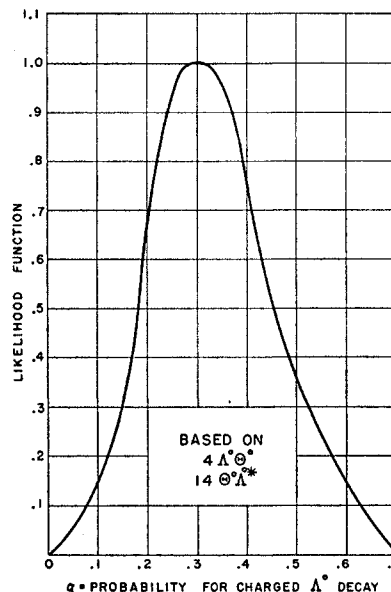


FIG. 12. The likelihood function is plotted against α , the probability for charged Λ^0 decay ($\Lambda^0 \rightarrow \pi^- + p$). The most probable value of α is $\bar{\alpha}_{\Lambda^0} = 0.3_{-0.12}^{+0.15}$. The asterisk denotes events in which only the θ^0 was observed.

lifetime is seen from Table III to be less than the statistical error.

VIII. LIFETIMES OF Λ^0 , θ^0 , Σ^-

The data requisite for calculating the lifetimes of the 23 observed Λ^0 's, 18 observed θ^0 's, and 17 Σ^- , are given in Tables I and II. A statistical analysis based on the

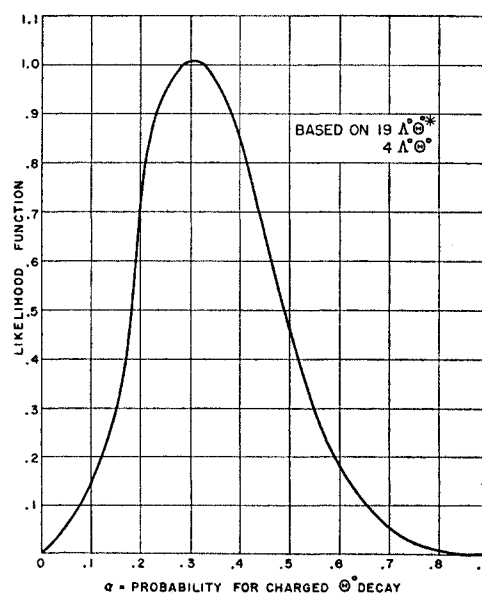


FIG. 13. The likelihood function is plotted against α , the probability for charged θ^0 decay ($\theta^0 \rightarrow \pi^+ + \pi^-$). The most probable value of α is $\bar{\alpha}_{\theta^0} = 0.3_{-0.12}^{+0.19}$. The asterisk denotes events in which only the Λ^0 was observed.

TABLE III. The variation of $\bar{\alpha}_{A0}$, $\bar{\alpha}_{\theta 0}$ with assumed lifetime.

$\tau_{A0} \times 10^{-10}$ sec	2.5	3	3.5
$\bar{\alpha}_{A0}$	0.28	0.3	0.32
$\tau_{\theta 0} \times 10^{-10}$ sec	1	1.25	1.5
$\bar{\alpha}_{\theta 0}$	0.25	0.3	0.35

methods of Bartlett¹⁶ gives

$$\tau_{A0} = (2.0_{-0.7}^{+1.3}) \times 10^{-10} \text{ sec},$$

$$\tau_{\theta 0} = (1.2_{-0.2}^{+0.6}) \times 10^{-10} \text{ sec},$$

which are in reasonable agreement with the best values given in Sec. VII. Poor statistics and small chamber size preclude the possibility of good lifetime measurement here. The Σ^- lifetime is obtained from the likelihood function:

$$L(\tau) = \prod_{i=1}^N \frac{e^{-t_i/\tau}}{\tau(1 - e^{-T_i/\tau})},$$

which is plotted against τ in Fig. 14. Notation is identical to that used in Sec. VII. The best value is

$$\tau_{\Sigma^-} = (1.4_{-0.5}^{+1.6}) \times 10^{-10} \text{ sec}.$$

The errors are statistical, taken from the width of $L(\tau)$ at half-maximum. To the best of our knowledge, this is the only Σ^- lifetime determination free from ambiguity in the charge of the decaying hyperon.

IX. MASS OF THE Σ^-

In one of the 16 cases of Σ^- decay (see Fig. 1), the π^- meson comes to rest. This permits a determination of the energy release in the decay $\Sigma^- \rightarrow \pi^- + n$. The Q value is calculated from a measurement of the π^- range, its angle of emission, and the velocity of the Σ^- before decay. Although the Σ^- velocity can be calculated from the measurements on the angles of K^+ and Σ^- production in this particular event, a more accurate value is obtained by using our information on the mean beam energy given in Sec. III. Using the values 1.433 ± 0.015 BeV/c for the momentum of the incident pion beam, 64.5° for the angle of production of the K^+ , the Σ^- velocity is $v/c = 0.742$. From the measured range 11.6 ± 0.2 cm of the decay π^- , the density 0.429 g/cm³, and the stopping power 2.49 MeV/g/cm³ of the propane, the kinetic energy of the decay pion is 24.9 ± 0.26 MeV. The angle of decay is measured to be $86.0 \pm 1^\circ$ in the

¹⁶ M. S. Bartlett, Phil. Mag. 44, 249 (1953).

laboratory system. Using these figures we get $Q(\Sigma^- \rightarrow \pi^- + n) = 118 \pm 2.6$ MeV. The corresponding decay for the Σ^+ hyperon has a $Q(\Sigma^+ \rightarrow \pi^+ + n) = 110 \pm 1$ MeV. It is to be noted that since Σ^- and Σ^+ are not charge conjugates, this mass difference, although unusually large for an electromagnetic mass, is not in conflict with any established theoretical considerations. The mass difference can be accounted for by the differences in the electromagnetic interactions of the virtual heavy particle currents in the self-energy calculation.

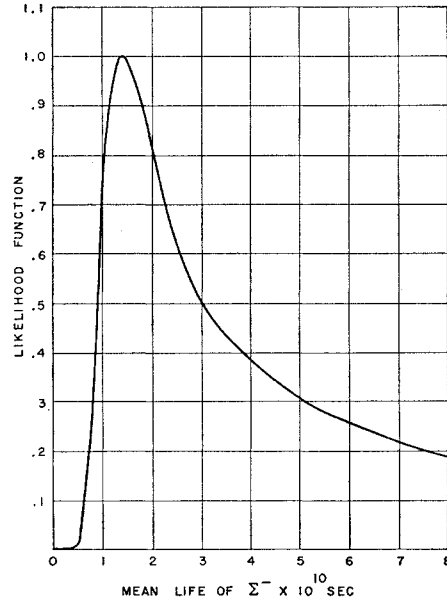


FIG. 14. The likelihood function is plotted against τ , the Σ^- lifetime. The most probable value for τ is $\tau_{\Sigma^-} = (1.4_{-0.5}^{+1.6}) \times 10^{-10}$ sec.

ACKNOWLEDGMENTS

We take this opportunity to express our thanks to Dr. D. Glaser for his help in the construction of the chamber, to Dr. E. Booth, Dr. L. Lederman, and Dr. R. Shutt for discussions on photographic techniques, and to the staff of the Cosmotron Department at the Brookhaven National Laboratory, in particular Dr. W. Moore, for assistance with the exposures. We would also like to express our gratitude for their invaluable aid to our scanners, Miss J. Chin and Mr. H. Shute, and to the staff of the I.B.M. machines at the Columbia University Hudson Laboratories in Dobbs Ferry, New York.

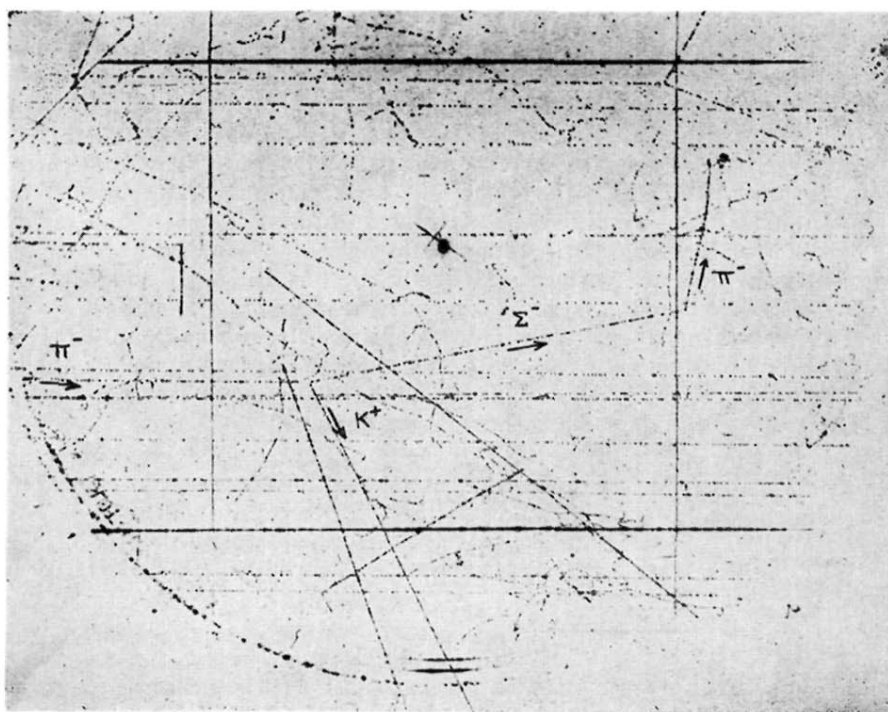


FIG. 1. $\pi^- + p \rightarrow \Sigma^- + K^+$, $\Sigma^- \rightarrow \pi^- + n$. The Σ^- decay product stops in the chamber and makes a star which shows a short proton recoil. It is therefore identified as a π^- .

FIG. 2. $\pi^- + p \rightarrow \Sigma^- + K^+$. here both the Σ^- and K^+ decay. The K^+ decay product itself decays into an electron, and is therefore identified as a μ^+ .

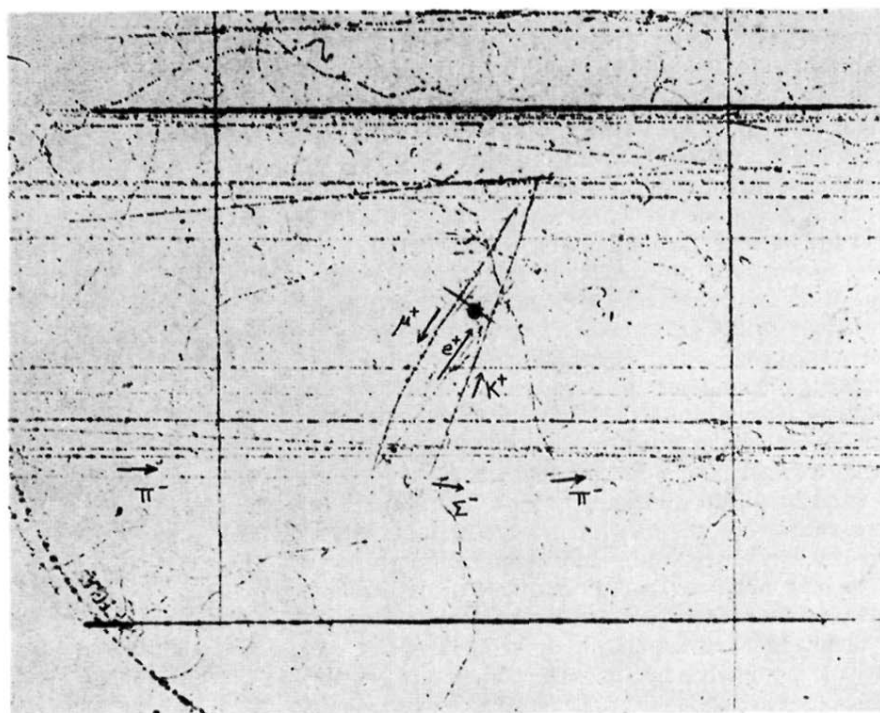
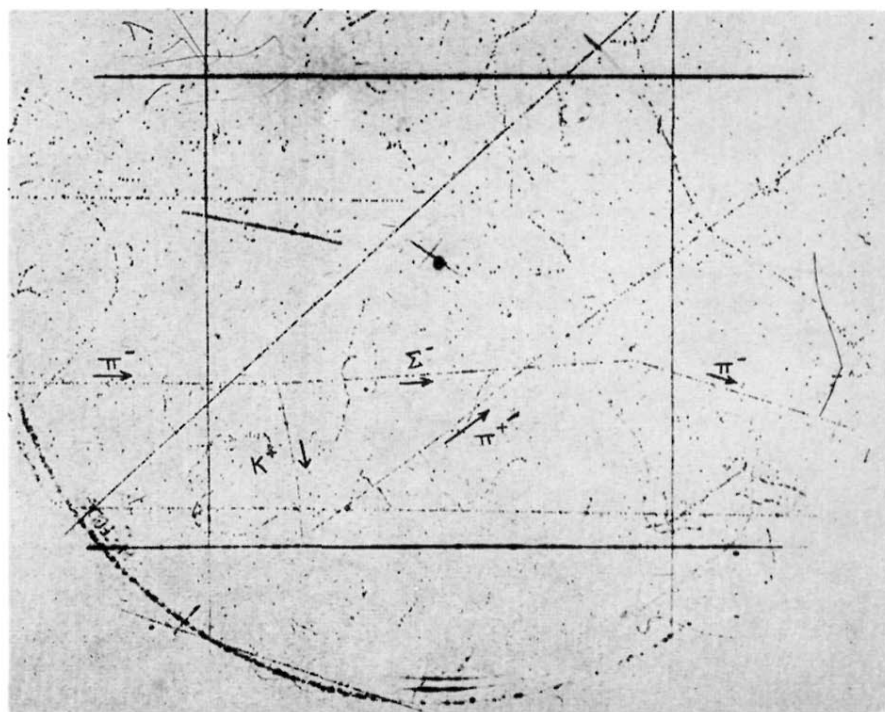


FIG. 3. $\pi^- + p \rightarrow \Sigma^- + K^+$. The K^+ decay product is minimum-ionizing and scatters severely, and is therefore identified as an electron. The electron was erroneously labeled π^+ and should read e^+ .



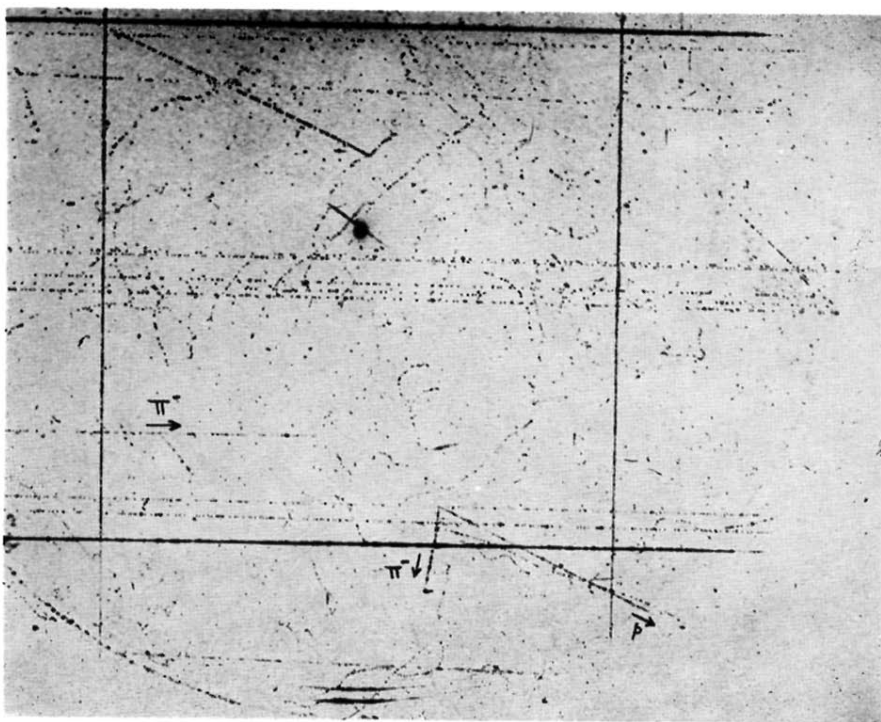


FIG. 4. A $\Lambda^0-\theta^0$ production in which only a single V is seen. The V is identified as a Λ^0 and shows a slow π^- producing a star.

FIG. 5. A Λ^0 - θ^0 production in which both V 's are seen. The Λ^0 shows, characteristically, a heavily ionizing proton and a minimum-ionizing π^- . The θ^0 shows two minimum-ionizing π 's.

